SCIENCE CHINA
Information Sciences

• **LETTER** •

August 2026, Vol. 69, Iss. 8, 180508:1–180508:2
https://doi.org/10.1007/s11432-026-5027-y

Special Topic: Quantum Information

The correlated matching decoder for the 4.8.8 color code

Yantong LIU, Junjie WU* & Lingling LAO*

College of Computer Science and Technology, National University of Defense Technology, Changsha 410073, China

Received 28 January 2026/Revised 2 May 2026/Accepted 30 June 2026/Published online 29 July 2026

Citation Liu Y T, Wu J J, Lao L L. The correlated matching decoder for the 4.8.8 color code. Sci China Inf Sci, 2026, 69(8): 180508, https://doi.org/10.1007/s11432-026-5027-y

Color codes present distinct advantages for fault-tolerant quantum computing, such as high encoding rates and the transversal implementation of Clifford gates. To fully exploit these properties in fault-tolerant architectures, high-performance decoding algorithms for color codes are indispensable. However, the restricted decoder [1]—a standard matching-based decoder for color codes, which decodes by applying minimum-weight perfect matching (MWPM) independently on two or three restricted lattices—cannot resolve certain weight-$O(d/2)$ diagonal error configurations on the 4.8.8 lattice, due to ignoring correlations between restricted lattices. Since the logical failure rate in the low-error regime is dominated by minimum-weight failure events, this limitation directly impacts decoding performance.

Inspired by the unified decoder [2] and the correlated surface code decoder [3], we introduce a correlated decoder for the 4.8.8 color code that leverages correlations between restricted lattices to resolve this problem. We provide two versions: v1 decodes on two restricted lattices (faster), and v2 decodes on all three lattices (more accurate). We analyze the decoding performance for the minimum-weight ($O(d/2)$) uncorrectable error chains, demonstrating exponential improvement over the restricted decoder at very low physical error rates. Our correlated decoders achieve higher thresholds than both the restricted and unified decoders under code-capacity and phenomenological noise, while matching the performance of the unified decoder at very low error rates with lower decoding time. Via the surface-color code mapping, our decoder also outperforms the correlated surface code decoder. Finally, we generalize the decoder to the circuit-level noise model.

Correlated Decoder. The conventional restricted decoder for the 4.8.8 color code functions by independently decoding on two of the three restricted lattices, $\mathcal{R}_{\mathbf{b}}$ and $\mathcal{R}_{\mathbf{g}}$. Here, $\mathcal{R}_{\mathbf{u}}$ denotes the restricted lattice obtained by removing all color-**u** checks. A limitation of this approach is that it cannot correct certain weight-$O(d/2)$ diagonal error configurations. This is because it cannot resolve the degeneracy between a combined vertical-horizontal weight-2 X error and a diagonal weight-2 X error on a red square, leading to an overestimation of the weight of the correct matching path. Under the color-surface code mapping, this is analogous to the inability of the independent X/Z MWPM decoder to resolve the degeneracy between a combined X-Z error and a Y error on a single qubit of the surface code.

The correlated MWPM decoder [3] for the surface code addresses this issue by setting the weight of edges identified in the first matching to zero during the second matching. This works because, under depolarizing noise, if a $Z(X)$ error occurs on a qubit, an $X(Z)$ error occurs on the same qubit with probability 1/2 (forming a Y error), corresponding to a weight-0 edge. Guided by the color-surface code mapping, we identify the core step of the correlated decoder (denoted v1) for the color code that addresses analogous issues. As shown in the left panel of Figure 1, for decoding the vertical logical Z operator, the procedure first decodes on the $\mathcal{R}_{\mathbf{b}}$ lattice (Figure 1(a)(ii)) and marks the red checks (deep red squares) fully traversed by matching edges, then sets the weights of edges (dashed lines) in the $\mathcal{R}_{\mathbf{g}}$ lattice (Figure 1(a)(iii)) incident to the marked red checks to zero before decoding on $\mathcal{R}_{\mathbf{g}}$. This correlated decoder successfully corrects the weight-$O(d/2)$ diagonal error configurations that the restricted decoder cannot resolve; examples are provided in the Supplementary Material.

The correlated procedure of v1 described above leverages correlations between $\mathcal{R}_{\mathbf{b}}$ and $\mathcal{R}_{\mathbf{g}}$ to resolve the degeneracy of two-qubit diagonal errors. However, correlations also exist in other error configurations and extend to the $\mathcal{R}_{\mathbf{r}}$ lattice (Figure 1(a)(i)). For instance, for certain error patterns such as adjacent diagonal errors and boundary error configurations, v1 may make an incorrect choice when decoding $\mathcal{R}_{\mathbf{b}}$, which can lead to failure when decoding $\mathcal{R}_{\mathbf{g}}$. To address this, we further improve the decoder (denoted v2) by incorporating decoding information from the $\mathcal{R}_{\mathbf{r}}$ lattice, which provides additional information from a different perspective. Specifically, based on the decoding results from $\mathcal{R}_{\mathbf{r}}$, we set the weights of edges (gray lines) associated with qubits (deep red) likely to be in error in both the $\mathcal{R}_{\mathbf{g}}$ and $\mathcal{R}_{\mathbf{b}}$ lattices to 0.999. The remaining procedures remain unchanged. This minor weight modification biases the decoder toward choosing the correct path, improving the handling of error patterns that v1 may fail to correct. More illustrative examples are shown in the Supplementary Material.

Compared to the restricted decoder, the correlated decoder v1 incurs no additional computational overhead but sacrifices decoding parallelism across restricted lattices. Correlated decoder v2 achieves better logical error rates by leveraging the redundant third restricted lattice, at the cost of one additional matching round.

Numerical results. In the regime of asymptotically low physical error rates, the logical error rate is mainly determined by the

* Corresponding author (email: junjiewu@nudt.edu.cn, laolinglingrolls@gmail.com)

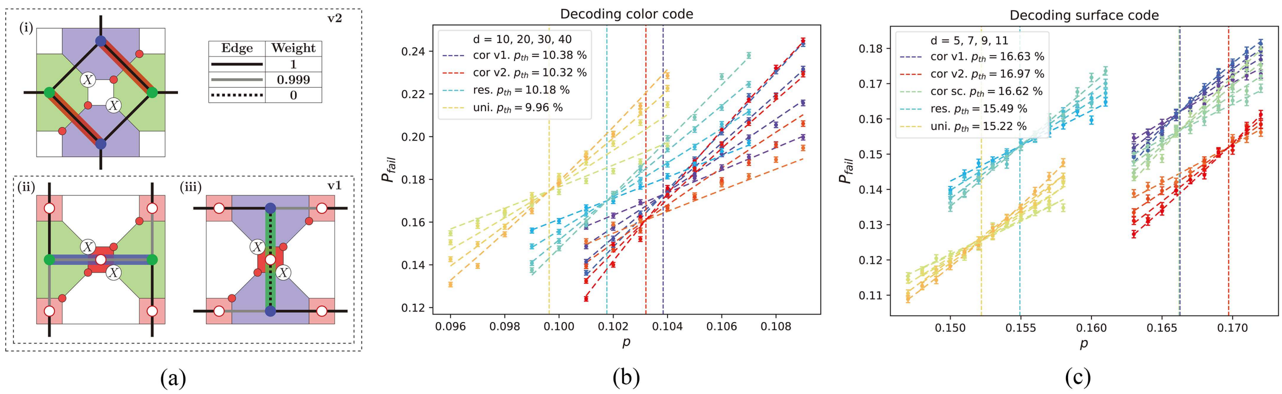

Figure 1 (Color online) (a) Decoding procedures of correlated decoder v1 and v2 (see text for details). Violated checks are highlighted as filled circles. Thin lines represent edges with assigned weights, and thick lines indicate the obtained matching. (b) and (c) Threshold comparison of the restricted, unified, and correlated decoders (v1, v2, and the correlated surface decoder labeled "cor sc") for decoding the color code and the surface code under the code-capacity noise model.

number of minimum-weight failure mechanisms. We evaluate the logical failure rates of correlated decoders at low physical error rates using the rare-event splitting method. Correlated decoder v1 achieves performance comparable to that of the unified decoder for weight-$d/2$ errors, while correlated decoder v2 achieves performance identical to that of the unified decoder.

We now analyze the decoding time of these decoders. The restricted decoder can decode on the restricted lattices in parallel, whereas the correlated decoder cannot. As a result, the restricted decoder is approximately $2\times$ ($3\times$) faster than the correlated decoder v1 (v2). The running time of PyMatching is linear in the number of nodes in the decoding graph at low error rates. The correlated decoder v1 (v2) performs MWPM on two (three) restricted lattices, while the unified decoder performs MWPM on a unified lattice connecting three restricted lattices. Consequently, the unified decoder requires approximately $1.5\times$ ($1\times$) the decoding time of the correlated decoder v1 (v2). However, as the physical error rate increases, the runtime of PyMatching becomes superlinear ($O(n^\alpha)$ with $\alpha > 1$), making the correlated decoder v2 faster than the unified decoder ($O(3n^\alpha)$ vs. $O(3^\alpha n^\alpha)$).

We also estimate thresholds using Monte Carlo simulations (10^5 samples per point). The threshold is calculated by fitting the logical error rate data to a Taylor expansion truncated to the quadratic term $f = Ax^2+Bx+C$, where $x = (p-p_{\rm th})^{1/\nu}$ is the rescaled error rate. Under the code capacity noise model, the correlated decoders achieve thresholds of 10.38% (v1)/10.32% (v2) for the color code (bit-flip error) and 16.63% (v1)/16.97% (v2) for the surface code (depolarizing error), as shown in Figure 1. Our correlated decoder v2 also outperforms the correlated surface code decoder, suggesting that the improvement from using the $\mathcal{R}_{\mathbf{r}}$ lattice can in turn benefit surface code decoding through the surface-color code mapping. Under the phenomenological noise model, the thresholds are 3.13% (v1)/3.23% (v2) for the color code and 3.51% (v1)/3.69% (v2) for the surface code.

Under the circuit-level noise model, our correlated decoder achieves a slight improvement over the restricted decoder and performs closely to the Chromobius decoder. This is expected because the error configurations whose decoding is improved by the correlated decoder no longer constitute the dominant source of logical failure in this regime. Instead, uncorrectable errors arise primarily from complex error mechanisms that effectively reduce the code distance under circuit-level noise, which fundamentally limits the performance of conventional matching-based decoders. Detailed data for all results above are provided in the Supplementary Material.

Conclusion and discussion. In this work, we introduce a correlated decoder for the 4.8.8 color code that enhances the restricted decoder by leveraging correlations between restricted lattices, thereby resolving the inconsistency between correction weight and matching weight. Our results demonstrate improvements over the restricted decoder under both code-capacity and phenomenological noise models. We note that conceptually similar strategies "over-matching" and "correlated symatching" in [4], and the concatenated decoder [5]—similarly leverage redundant symmetries and correlations, further supporting the broad value of this principle in matching-based decoding.

Our correlated decoder also provides a new perspective that can improve surface-code decoding: the matching on the $\mathcal{R}_{\mathbf{r}}$ lattice maps to X-Z hybrid matching on the surface code. This preliminary idea is worth developing and testing in future work. Looking forward, developing a more general correlated decoding framework remains an important direction, as our current re-weighting strategy becomes less effective under circuit-level noise due to its complex error mechanisms and rigid edge weights. Extending this principle to other code families also constitutes a promising future direction.

Acknowledgements This work was supported by National Key R&D Program of China (Grant No. 2024YFB4504001), National Natural Science Foundation of China (Grant Nos. 62302395, 62421002), Fundamental and Interdisciplinary Disciplines Breakthrough Plan of the Ministry of Education of China (Grant No. JYB2025XDXM202), and Aid Program for Science and Technology Innovative Research Team in Higher Educational Institutions of Hunan Province. We acknowledge support from the QUANTA (Quantum Fans from IT Area) group.

Supporting information Appendixes A–E. The supporting information is available online at info.scichina.com and link.springer.com. The supporting materials are published as submitted, without typesetting or editing. The responsibility for scientific accuracy and content remains entirely with the authors.

References

1 Kubica A, Delfosse N. Efficient color code decoders in $d \geqslant 2$ dimensions from toric code decoders. Quantum, 2023, 7: 929
2 Benhemou A, Sahay K, Lao L, et al. Minimising surface-code failures using a color-code decoder. Quantum, 2025, 9: 1632
3 Delfosse N, Tillich J P. A decoding algorithm for CSS codes using the x/z correlations. In: Proceedings of 2014 IEEE International Symposium on Information Theory, 2014. 1071–1075
4 Sahay K, Williamson D J, Brown B J. A matching decoder for bivariate bicycle codes. ArXiv:2602.22770
5 Lee S H, Li A, Bartlett S D. Color code decoder with improved scaling for correcting circuit-level noise. Quantum, 2025, 9: 1609